An *in vitro* and *in vivo* efficacy evaluation of gene therapy candidate SBT101 in mouse models of adrenomyeloneuropathy and in NHPs

Vidyullatha Vasireddy,[1,11] Casey A. Maguire,[2,3] David W. Anderson,[1,11] Carrie Ng,[2,3] Yi Gong,[2,3] Florian Eichler,[2,3] Stéphane Fourcade,[4,5] Cristina Guilera,[4,5] Andrea Onieva,[6,7] Angela Sanchez,[6,7] Marc Leal-Julià,[6,7] Sergi Verdés,[6,7] Inge M.E. Dijkstra,[9] Stephan Kemp,[9] HongGeun Park,[1,12] Tiffany Lutz,[1,13] Sean W. Clark,[1,14] Assumpció Bosch,[6,7,8] Aurora Pujol,[4,5,10] and Karen Kozarsky[1,15]

[1]SwanBio Therapeutics, Inc., Philadelphia, PA, USA; [2]Department of Neurology, Massachusetts General Hospital, Charlestown, MA, USA; [3]Harvard Medical School, Boston, MA, USA; [4]Neurometabolic Disease Laboratory, Instituto de Investigación Biomédica de Bellvitge (IDIBELL), Hospital Duran i Reynalds, Barcelona, Spain; [5]Centre for Biomedical Research on Rare Diseases (CIBERER), Instituto de Salud Carlos III (ISCIII), Madrid, Spain; [6]Department of Biochemistry and Molecular Biology and Institute of Neurosciences, Universitat Autònoma de Barcelona, Barcelona, Spain; [7]Unitat Mixta UAB-VHIR, Vall D'Hebron Institut de Recerca (VHIR), Barcelona, Spain; [8]Centro de Investigación Biomédica en Red Sobre Enfermedades Neurodegenerativas (CIBERNED), Instituto de Salud Carlos III (ISCIII), Madrid, Spain; [9]Laboratory Genetic Metabolic Diseases, Department of Laboratory Medicine, Amsterdam UMC location University of Amsterdam, Amsterdam Neuroscience, Amsterdam Gastroenterology Endocrinology Metabolism, Amsterdam, the Netherlands; [10]Catalan Institution of Research and Advanced Studies (ICREA), 08010 Barcelona, Catalonia, Spain

Adrenomyeloneuropathy is a progressive neurodegenerative disease caused by pathogenic variants in the *ABCD1* gene, resulting in very-long-chain fatty acid (VLCFA) accumulation that leads to dying-back axonopathy. Our candidate gene therapy, SBT101 (AAV9-human *ABCD1* [h*ABCD1*]), aims to ameliorate pathology by delivering functional copies of h*ABCD1* to the spinal cord. Transduced cells produce functional ABCD1 protein, thereby repairing the underlying biochemical defect. *In vitro* and *in vivo* mouse studies were conducted to assess the biochemical and functional efficacy of SBT101 and show effective delivery to target tissues involved in the disease pathology: spinal cord and dorsal root ganglia. Administration of SBT101 to mixed glial cell cultures from *Abcd1*-Null mice, and to male *Abcd1* knockout (*Abcd1*$^{-/y}$) and double-knockout (*Abcd1*$^{-/y}$/*Abcd2*$^{-/-}$) mice led to increased hABCD1 production and reduced VLCFA. Double-knockout mice also exhibited improved grip strength. Furthermore, we conducted biodistribution and safety assessments in nonhuman primates. Six-hour intrathecal lumbar infusions demonstrated effective transduction throughout target tissues, supporting the clinical feasibility of the procedure. SBT101 was well tolerated, with no observed SBT101-related mortality or clinical signs. These findings not only provide preclinical efficacy data for SBT101 but also inform clinically relevant SBT101 dose selection for patients with adrenomyeloneuropathy.

INTRODUCTION

Adrenomyeloneuropathy (AMN) is a debilitating and progressive inherited neurodegenerative disease that primarily affects the spinal cord and often the adrenal glands.[1,2] It is caused by pathogenic mutations in the adenosine triphosphate-binding cassette sub-family D member 1 (*ABCD1*) gene, leading to a deficiency in the ABCD1 protein.[3,4] *ABCD1* encodes a peroxisomal membrane protein that transports acylated very-long-chain fatty acids (VLCFAs) as coenzyme A (CoA) esters from the cytosol into the peroxisome for degradation.[3] ABCD1 is a half transporter and requires a partner half-transporter molecule to form a functional homodimeric or heterodimeric transporter.[5,6] Pathogenic variants in *ABCD1* lead to deficient peroxisomal degradation of VLCFAs and their accumulation in both plasma and tissues, affecting function in adrenal glands, testes, and the central nervous system (CNS). VLCFA accumulation causes oxidative stress and mitochondrial impairment at the cellular level and progressive axonopathy in the spinal cord.[3,7,8] The VLCFA profile is considered to be a reliable diagnostic marker of AMN and plays a role in intracellular pathogenesis[3,7,8]; however, trials have shown that AMN progresses even when plasma levels of VLCFAs are normalized,[9] indicating that VLCFA levels need to be reduced in the affected tissues.

Males (particularly boys) are at risk to develop adrenal insufficiency and/or inflammatory cerebral demyelination.[9] In adulthood, the core manifestation of ABCD1 deficiency is myeloneuropathy.[3,10] Symptoms typically occur in adulthood, affecting virtually all men and more than 80% of women with a pathogenic variant.[1,8,11] Males (particularly boys) may also develop additional complications, such as urinary and bowel incontinence, as well as adrenal insufficiency and/or inflammatory cerebral demyelination.[9] While there is hormone replacement for the patient suffering from adrenal insufficiency, no treatment for the neurological symptoms exists. Adult patients typically experience slowly progressing spinal cord disease affecting sensory ascending and motor descending spinal cord tracts characterized by dying-back axonopathy that leads to sensory ataxia and progressive spastic paraplegia, loss of mobility, incontinence, debilitating pain, and sexual dysfunction.[1,12,13] Over time, AMN confers a high and increasing burden on the patients and their families, leading to permanent disability and pervasive, difficult-to-manage symptoms that significantly affect quality of life.[1,12,14] In the current absence of effective therapies, patients experience progressive neurodegeneration.[9]

Gene therapy is a promising therapeutic approach that could address the current lack of effective treatments for AMN, offering the potential to modify the underlying causes of the disease and provide long-lasting improvements after a single treatment. One such therapeutic approach under investigation is the use of adeno-associated virus (AAV)-mediated gene replacement. This approach aims to deliver a functional copy of human *ABCD1* (h*ABCD1*) to the spinal cord that would then induce recipient cells to produce the hABCD1 protein, thus partially or fully correcting the biochemical defects that underlie AMN. Two proof-of-concept studies in mouse models of human AMN have demonstrated that intrathecal administration of an AAV9-h*ABCD1* construct (SBT101) was able to reduce VLCFA levels.[15,16] Recombinant AAV9 was selected as the vector due to it being an established gold standard for vector-mediated gene therapy in CNS disorders with its wide biodistribution in the brain and spinal cord.[17] In addition to examining the administration route, these studies also examined infusion speed as an important factor for optimizing SBT101 delivery. Slow intrathecal administration using an osmotic pump was associated with lower systemic leakage of SBT101, especially to the heart and liver, than intrathecal bolus administration.[16] Taken together, these prior mouse studies demonstrated the biodistribution and persistence of vector genomes following administration, thereby reinforcing the applicability of a viral platform for therapeutic gene delivery. Based on these two preclinical mouse studies,[15,16] an AAV9-h*ABCD1* construct (SBT101) was characterized and subsequently optimized for clinical development. Clinical studies using AAV-mediated gene therapy have demonstrated sustained transgene expression, functional response, and a promising safety profile in patients with CNS diseases. These diseases have included Parkinson's disease,[17,18] Canavan disease,[19] late infantile neuronal ceroid lipofuscinosis,[20] and giant axonal neuropathy (ClinicalTrials.gov identifier NCT02362438).

An important first step to consider with any gene therapy is how it will be administered such that the treatment reaches the tissues involved in the disease pathology. With AMN, the target tissues for transduction are the spinal cord and dorsal root ganglia (DRG). Several administration routes (intracerebroventricular, intravenous, and intrathecal) have been previously investigated for the delivery of AAV-based constructs in mice. Intravenous administration of an AAV serotype 9 (AAV9)-h*ABCD1* construct in male hemizygous *Abcd1* knockout mice (human adrenoleukodystrophy model) was associated with widespread hABCD1 expression throughout the CNS,[15] while intracerebroventricular administration of an AAV-interferon beta construct in mice led to localized expression in the injected ventricle.[15,21] Despite the capacity for widespread tissue transduction, intravenous administration requires large doses of recombinant AAV9, which increases the likelihood of toxicity.[16] Compared with intravenous administration, intrathecal administration has the potential to offer a narrower delivery profile, with transduction targeted to the specific tissues involved in AMN pathology. Indeed, studies across several species have shown greater recombinant AAV vector-based transduction of the spinal cord and DRG with intrathecal versus intravenous administration, and at 10-fold lower doses.[22,23]

Owing to the differences between rodents and humans, such as size and spinal cord biology, it is important to bridge this gap by evaluating SBT101 administration routes and infusion parameters in animal models more akin to humans. Nonhuman primates (NHPs), particularly cynomolgus macaques, are often used in biomedical research to bridge this species gap.[24] In addition to enabling the evaluation of SBT101 biodistribution in a model more closely reflective of humans, NHPs have similar pharmacological responses to humans, which allows toxicological assessments of SBT101 in a system more representative of humans than mice. Moreover, the target tissues for SBT101 therapy, spinal cord and DRG, are anatomically similar between NHPs and humans, and the upright posture of NHPs provides a better model of cerebrospinal fluid (CSF) flow than rodents.

Here, we describe our preclinical findings on the biochemical and functional efficacy of SBT101 in a series of *in vitro* and *in vivo* mouse studies to establish a minimally effective dose. Combined with an evaluation of the biodistribution and safety of SBT101 in cynomolgus macaques, these findings were used to inform suitable SBT101 doses for the PROPEL trial (ClinicalTrials.gov identifier NCT05394064), a first-in-human study.

RESULTS

SBT101 in mixed glial cell cultures from *Abcd1*-Null mice

Significant dose-dependent expression of hABCD1 was observed in mixed glial cell cultures following treatment with SBT101 at 3.3E4 vector genomes/cell (vg/cell) ($p < 0.05$), 1.0E5 vg/cell ($p < 0.0001$), and 3.3E5 vg/cell ($p < 0.0001$) compared with phosphate-buffered saline (PBS)-treated control cultures from *Abcd1*-Null mice (Figure 1A).
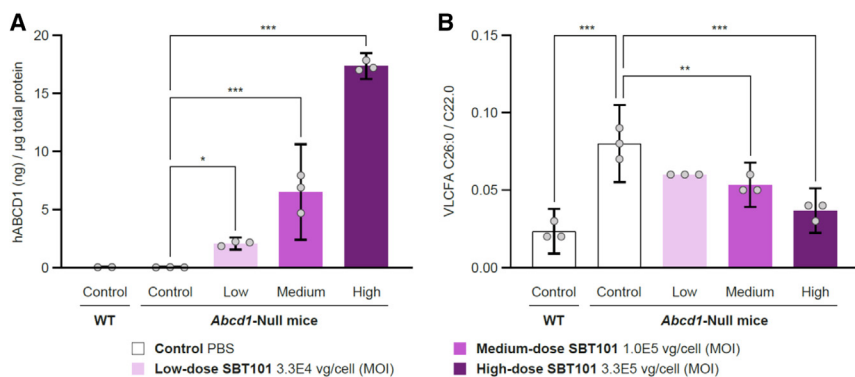
Figure 1. Increased hABCD1 expression and VLCFA reduction in mixed glial cell cultures following SBT101 administration

Human ABCD1 expression (A) and VLCFA levels (B) in mixed glial cell cultures (from *Abcd1*-Null and WT mice) exposed to SBT101. $*p < 0.05$, $**p < 0.01$, $***p < 0.0001$. Data represent mean ±95% confidence interval.

VLCFA accumulation was evident in the mixed glial cells obtained from *Abcd1*-Null mice compared with wild-type (WT) cells. Treatment with SBT101 led to dose-dependent reductions in VLCFA levels compared with PBS-treated control cultures from *Abcd1*-Null mice (Figure 1B). This reached statistical significance at SBT101 doses of 1.0E5 ($p < 0.01$) and 3.3E5 vg/cell ($p < 0.0001$).

SBT101 in $Abcd1^{-/y}$ mice

In an 8-week dose-finding study (mouse *in vivo* study 1), mice aged 20–23 months received intrathecally administered SBT101 or formulation buffer control. SBT101 dose-dependent increases of viral genomes were observed, reaching statistical significance at 2.0E10 vg/animal (an) ($p < 0.0001$ vs. formulation buffer controls) (Figure 2A). Similarly, there were dose-dependent increases in hABCD1 expression within the spinal cord, which again reached significance at 2.0E10 vg/an ($p < 0.01$) (Figure 2B). No measurable hABCD1 expression was observed in either WT or $Abcd1^{-/y}$ mice receiving control treatment. Compared with WT animals, $Abcd1^{-/y}$ mice receiving control treatment had significant VLCFA accumulation in their spinal cord tissues ($p < 0.0001$). No significant differences were observed in VLCFA levels in $Abcd1^{-/y}$ mice receiving SBT101 at 2.0E10 vg/an versus control treatment (Figure 2C). This lack of reduction in VLCFA levels with SBT101 may have been due to the short 8-week mouse study period providing insufficient time for hABCD1 expression to significantly modify the slow turnover of VLCFA *in vivo*. In our studies, at least 3 months post injection was needed to detect significant lowering of VLCFA in the spinal cords of mice (see below). It is also possible that the advanced age of the mice contributed to the inability to detect a change in the 8-week study period, due either to further accumulation of VLCFA or slowing of metabolism with age. Finally, significant increases in mitochondrial DNA (mtDNA) copy numbers were recorded in the spinal cord of $Abcd1^{-/y}$ mice treated with SBT101 at 2.0E10 vg/an ($p < 0.05$ vs. control treatment), bringing levels in $Abcd1^{-/y}$ mice closer to those observed in WT mice (Figure 2D).

In a second mouse *in vivo* dose-finding study in which $Abcd1^{-/y}$ mice (aged 9–12 months) were observed for a longer duration (13 and 24 weeks) than mouse *in vivo* study 1, all but four of the 22 mice receiv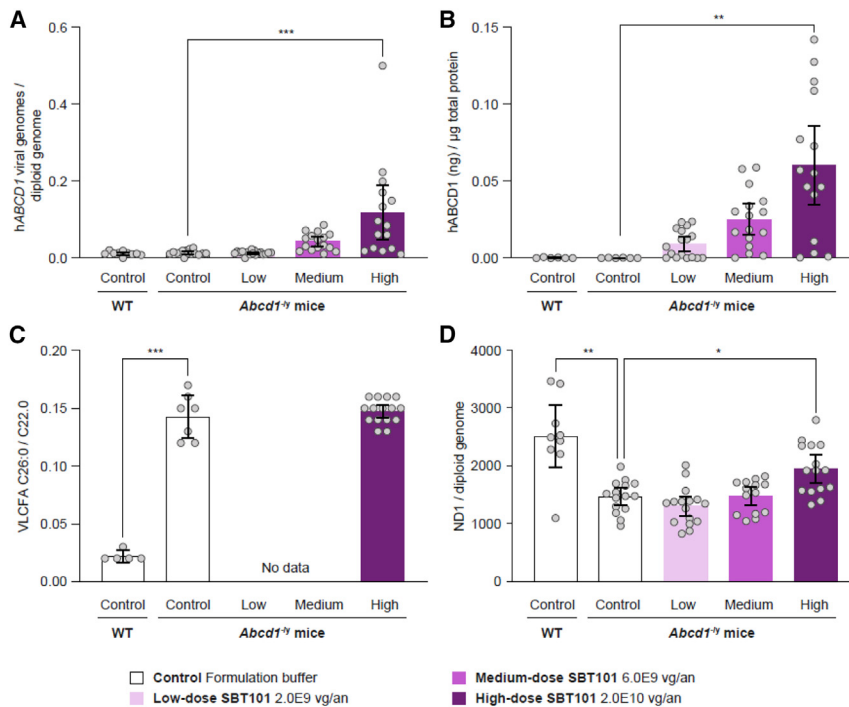ing SBT101 at 5.5E11 vg/an had died or required euthanasia before 13 weeks, and the four surviving mice were euthanized at the 13-week time point. Thus, data are not shown for this group. Post-mortem analysis indicated high transgene expression in the hearts of mice receiving 5.5E11 vg/animal, and histopathologic evidence of inflammation (data not shown). This level of transgene expression and the histopathologic findings in the heart appears specific to mice, as it was not observed in NHPs (see below).

$Abcd1^{-/y}$ and WT mice administered control treatment (formulation buffer) had no detectable viral genome copies in relation to *RPP30* (ribonuclease P/MRP subunit p30) in spinal cord tissue at either 13 or 24 weeks (Figures 3A and 3E, respectively). Mice administered SBT101 at 5.5E10 vg/an or 1.6E11 vg/an showed dose-dependent increases in viral genome copies, which reached statistical significance with 1.6E11 vg/an at 24 weeks ($p < 0.05$ vs. control treatment). Similarly, there were dose-dependent increases in hABCD1 protein expression in $Abcd1^{-/y}$ mice administered SBT101, but these did not reach statistical significance compared with control treatment (Figures 3B and 3F). With regard to VLCFA levels, there was significant accumulation in the spinal cord tissue of $Abcd1^{-/y}$ mice receiving control treatment compared with WT animals at 13 and 24 weeks post administration ($p < 0.0001$; Figures 3C and 3G, respectively). SBT101 at 1.6E11 vg/an led to significant reductions in VLCFA levels at 13 weeks ($p < 0.05$) and 24 weeks ($p < 0.01$) compared with control $Abcd1^{-/y}$ mice. mtDNA copy numbers in $Abcd1^{-/y}$ mice were lower than those in WT mice by 24 weeks, but the difference was not statistically significant. No significant changes in mtDNA copy numbers were observed in $Abcd1^{-/y}$ mice administered SBT101 or control treatment at 13 or 24 weeks post administration (Figures 3D and 3H, respectively).

Based on the findings across both mouse *in vivo* dose-finding studies, the minimum effective dose in mice was considered to be 2.0E10 vg/an (Figures 2A–2D), as this was the lowest dose that resulted in a significant change in an *in vivo* biochemical marker of ABCD1 function.

SBT101 in $Abcd1^{-/y}/Abcd2^{-/-}$ double-knockout mice

In a third mouse *in vivo* study, $Abcd1^{-/y}/Abcd2^{-/-}$ double-knockout (DKO) mice were utilized due to this model's earlier and more severe disease compared with single-knockout mice. ABCD2, the closest paralog to ABCD1, can compensate for ABCD1 deficiency because of the functional overlap between the two proteins.[25] DKO mice were administered intrathecal SBT101 or control AAV9-Null vector at 7–8 months of age. At 18 months of age, biodistribution of viral

Figure 2. Increased levels of hABCD1 and mtDNA, and reduced VLCFA levels, in *Abcd1*⁻/y mice 8 weeks after SBT101 administration

Viral genomes copy number (A), hABCD1 expression (B), VLCFA levels (C), and mtDNA levels (D) within the spinal cord of *Abcd1*⁻/y mice assessed at 8 weeks after SBT101 administration. *$p < 0.05$, **$p < 0.01$, ***$p < 0.0001$. Data represent mean ± 95% confidence interval.

mice given SBT101 at 3.3E10 vg/an or 3.3E11 vg/an showed a significant but non-dose-dependent increase in or prevention of loss of grip strength ($p < 0.01$) compared with control DKO mice receiving AAV9-Null vector (Figure 5). In these animals, grip strength was similar to that measured in control WT mice.

Biodistribution in cynomolgus macaques

A summary of the following NHP studies can be found in Table S1. To determine the effects of administration route and infusion rate on biodistribution, NHPs were administered an AAV9 vector with a green fluorescent protein (GFP) reporter gene, utilizing either lumbar or cervical intrathecal administration and comparing bolus to delivery infused over 24 h in NHP study 1. Doses were extrapolated based on CSF volume, given the compartment for delivery is the CSF. NHPs have ~325 times more CSF than mice; initial doses in NHPs were selected to be above the minimum effective dose in mice. The 24-h infusion resulted in widespread biodistribution of vector genomes across the entire spinal cord and DRG at 2 weeks after infusion as compared with the bolus delivery (Figure 6A). This effect was evident in all four administration groups based on a 20-min bolus lumbar infusion (1.06E13 vg/an), a 24-h lumbar infusion (1.26E13 or 3.38E13 vg/an), or a 24-h cervical infusion (1.20E13 vg/an). Immunohistochemical quantification of neuron positivity, in contrast to vector genomes, distinguished between the different routes of administration. This identified GFP expression in 25%–100% of cells (grades 3–5) in various locations within the spinal cord and DRG of tested animals (Figure 6B). Notably, only 24-h lumbar infusion resulted in GFP expression in the cervical spinal cord (Figure 6B), demonstrating the value of analyzing transgene expression in addition to vector genome localization. Use of a 3-fold higher dose of AAV with 24-h lumbar infusion did not generally result in transduction of additional regions of the CNS but did result in a higher proportion of cells with GFP expression (Figure 6B) and a higher intensity of GFP expression (data not shown). Given that broader transgene expression throughout the spinal cord and DRG is desirable for treating AMN, the 24-h lumbar infusion was investigated further.

genomes was widespread within the lumbar, thoracic, and cervical spinal cord of DKO mice (Figure 4A), and this was associated with SBT101 dose-dependent increases in h*ABCD1* mRNA expression (Figure 4B). Wide viral genome variation within the lumbar spinal cord was most probably due to a small number of outliers, likely as the result of the dosing solution being directly injected into the spinal cord rather than the intrathecal space. VLCFA levels in the lumbar spinal cord of DKO mice were higher than those in WT controls (Figure 4C). SBT101 was associated with dose-dependent reductions in VLCFA levels compared with control in DKO mice, but this did not achieve statistical significance, likely due to the limited number of spinal cords available for this analysis.

Immunohistochemical visualization of hABCD1 protein expression showed qualitative SBT101 dose-dependent increases in the thoracic spinal cord and thoracic DRG (Figure S1). Cells exhibiting hABCD1 expression also labeled positively for several CNS cell types, including neurons and astrocytes.

Levels of mRNA for the inflammatory cytokine tumor necrosis factor alpha (TNF-α), assessed in the lumbar spinal cord, were significantly increased in DKO mice compared with WT animals receiving control AAV9-Null vector ($p < 0.01$) (Figure 4D). SBT101 administration was associated with dose-dependent reductions in TNF-α mRNA levels that reached statistical significance at 3.3E11 vg/an ($p < 0.05$) and approached WT levels.

Grip strength was assessed in mice at 15 months of age, approximately 8 months post SBT101 administration, respectively. DKO
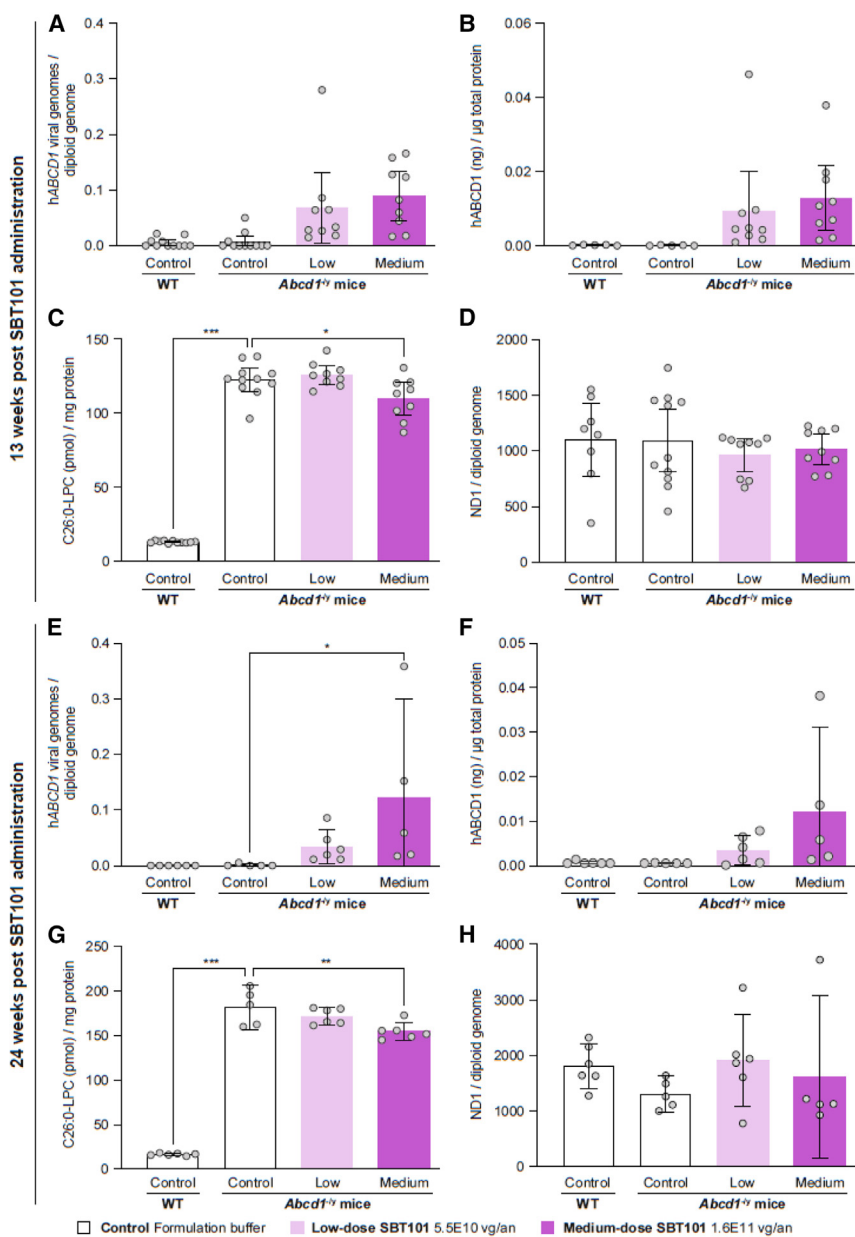
Considering the logistics of delivering vector to patients over 24 h, a second NHP biodistribution study (NHP study 2) was performed to examine whether a shorter infusion period would yield similar results

Figure 3. Increased levels of hABCD1 and mtDNA, and reduced VLCFA levels in *Abcd1⁻/y* mice at 13 and 24 weeks after SBT101 administration

Viral genomes copy number (A and E), hABCD1 expression (B and F), VLCFA levels (C and G), and mtDNA levels (D and H) within the spinal cord of *Abcd1⁻/y* mice assessed at 13 weeks (A–D) and 24 weeks (E–H) after SBT101 administration. $*p < 0.05$, $**p < 0.01$, $***p < 0.0001$. Data represent mean ± 95% confidence interval.

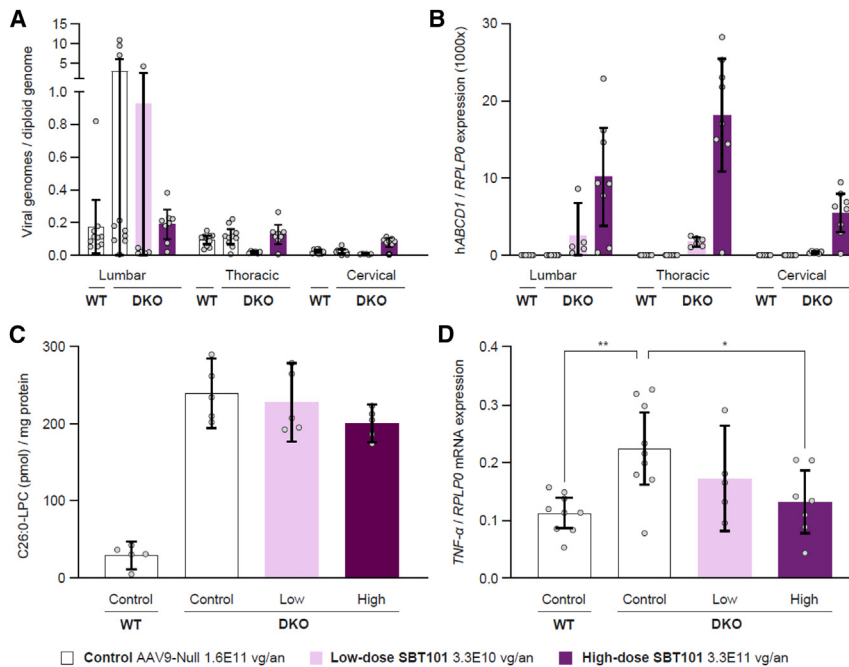## Safety in cynomolgus macaques

When the therapeutic vector, AAV9-hABCD1, was optimized, and both efficacy and dose selection established in mouse models, safety assessments were performed in NHPs. Three studies were conducted following a single 6-h intrathecal lumbar infusion of SBT101 at varying doses (7.77E12–7.62E13 vg/an) or vehicle control. Animals were followed for up to 12 months to assess the reversibility or persistence of any effects. NHP study 3 was a 6-month non-GLP study; NHP study 4 was a 6-month GLP study, and NHP study 5 was a GLP study that extended observations to 12 months. A summary of NHP studies can be found in Table S1.

Efficient transduction of target tissues was observed with detectable levels of both the vector genome and h*ABCD1* messenger RNA (mRNA) expression in DRG and spinal cord tissues (Figures 7, S9, and S10). Detectable levels were dose dependent and maintained from 1 to 12 months post SBT101 administration. Vector genome and h*ABCD1* mRNA levels were below the limit of detection for the vast majority of control animals (data not shown). Similar findings were observed across a variety of other tissues including brain, heart, and liver Figures S11–S13).

Neutralizing antibodies (NAbs) against AAV9 were first detected in sera on day 7 and generally remained elevated through day 183 (6 months; NHP studies 3 and 4) and day 365 (12 months; NHP study 5); however, there was no clear pattern of dose dependency in the relative NAb levels (Figures S2, S5, and S6). Few to no NAbs were detected in the sera of control animals. In CSF samples, AAV9 NAbs were first detected on day 56 in NHP study 3 and day 21 in NHP studies 4 and 5, but these were transient and not dose dependent (Figures S2, S5, and S6). Titers of NAbs in CSF were substantially lower than those in sera.

SBT101 was tolerated at all dose levels (up to 7.62E13 vg/an), with no drug-related effects on clinical, ophthalmological, or neurobehavioral observations; on vital signs, hematology, coagulation, or CSF tests; or

and whether the volume/rate of administration would have an effect. In this study, one condition from the first biodistribution study was repeated for comparison, the 24 h lumbar infusion. This study evaluated intrathecal lumbar infusion of the AAV9 vector with a GFP reporter gene at a single target dose (3.25E13 vg/an) and determined that GFP copy numbers and neuron positivity (defined as up to 50% of neurons expressing GFP) were similar between 6- and 24-h infusions and among dosing volumes of 2.5, 5.0, and 10.0 mL (Figure S4). The 6-h/5.0-mL infusion was selected for further development to enable a better patient experience, and a flow rate (up to ∼0.8 mL/h in NHPs, ∼8 mL/h in humans) that is considered safe and is not expected to increase CSF pressure.

Figure 4. Biochemical improvements following SBT101 administration in *Abcd1*$^{-/y}$/*Abcd2*$^{-/-}$ DKO mice

Viral genome distribution (A) and hABCD1 mRNA expression (B) in the spinal cord of *Abcd1*$^{-/y}$/*Abcd2*$^{-/-}$ DKO mice at 18 months of age (approximately 11 months after SBT101 administration). VLCFA levels (C) and inflammatory cytokine TNF-α levels (D) in the lumbar spinal cord of *Abcd1*$^{-/y}$/*Abcd2*$^{-/-}$ DKO mice at 18 months of age. $*p < 0.05$, $**p < 0.01$. Data represent mean ± 95% confidence interval.

NHPs receiving high-dose SBT101 were sacrificed at 3 months. Other observations reported at 3 months were commonly noted at 6 months but at an incidence and severity similar to control animals and were therefore considered to be background.

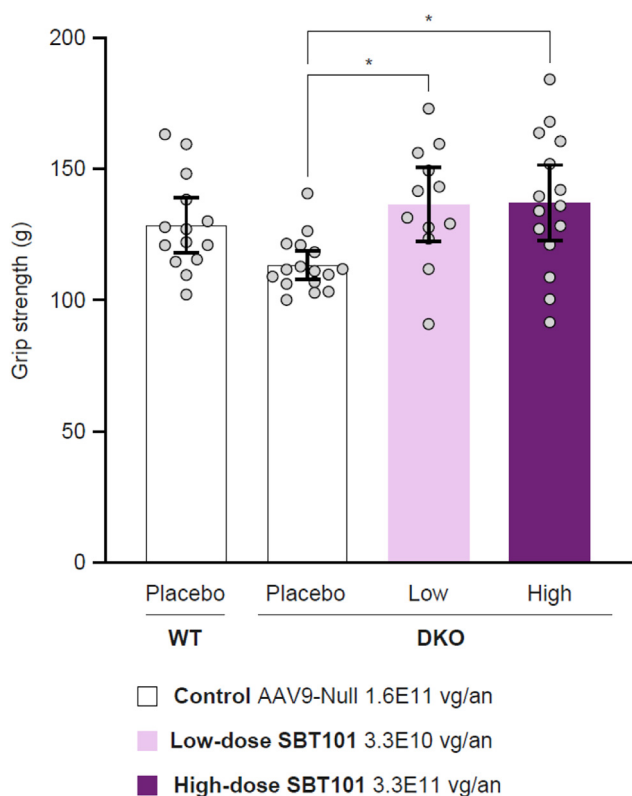Microscopic histopathological findings in NHP study 4 and NHP study 5 were similar to those observed in NHP study 3 (Figures S3, S7, and S8). Briefly, in NHP study 4, minimal to moderate axonal degeneration, neuronal necrosis, and mononuclear infiltrate were observed in the DRG, spinal cord, and peripheral nerves at 1 and 3 months (Figure S3). These observations were not dependent on SBT101 dose. At 6 months in the spinal cord, observations were mostly limited to minimal to moderate axonal degeneration. All other observations were of an incidence and severity similar to those in control animals and were considered to be background. In NHP study 5, at 12 months, treatment-related observations included slight axon degeneration and slight gliosis in the brain and moderate axonal degeneration in the spinal cord (Figure S8). In addition, minimal to moderate axonal degeneration and slight to moderate mononuclear infiltrate were observed in the DRG, minimal neuronal necrosis was noted in the lumbar DRG, and minimal to moderate axonal degeneration was recorded in the peripheral nerves. However, all 12-month histopathological findings were considered spontaneous and randomly distributed across groups (including control animals) and were as expected for male cynomolgus macaques of their age. Consequently, these observations were not considered related to treatment. Histopathological observations of the two animals that were sacrificed early (early deaths in Figure S8) showed minimal to moderate axon degeneration and mononuclear cell infiltration in the brain, spinal cord, DRG, and peripheral nerves. While there were no concurrent controls for these early sacrifices, the range of histopathology was generally consistent with observations made at the surrounding time points.

It is notable that transgene expression was detectable in target tissues and some off-target tissues through 12 months, indicating that long-term expression in target tissues is feasible. Transgene expression was not associated with any detectable negative outcomes in clinical observations, clinical chemistries, or with histopathologic safety signals.

during physical and electrocardiogram examinations (data not shown). Administration of SBT101 in NHP studies 3 and 4 was associated with transient, dose-dependent, mildly to moderately increased alanine aminotransferase (ALT) (Figures 8 and S14A), and transient, minimally to mildly increased aspartate aminotransferase (AST) activity (Figures 8B and S14B). In NHP study 5, transient, minimally to mildly increased ALT and AST levels were also observed (Figure S15). All increases were generally more pronounced between days 7 and 28 but were observed in individual animals up to day 92 for ALT and day 56 for AST. Levels had returned to normal without intervention by the time of terminal sacrifice in each study.

No drug-related mortality was observed. Two NHPs that were administered high-dose SBT101 (4.00E13 vg/an) in NHP study 5 were euthanized on days 76 and 140 owing to self-mutilation and severe liquid feces, respectively; these events were not considered related to the treatment.

Microscopic observations were made of the DRG, spinal cord, and peripheral tissues post SBT101 administration using a grading scale of 0 (unremarkable) to 5 (severe). In NHP study 3, minimal to moderate (grades 1–3) histopathological findings were observed in target tissues (DRG and spinal cord) in all dosed animals at 3 months, irrespective of dose level (Figure S7). SBT101-related neuronal necrosis was minimal to moderate and was characterized by nerve cell bodies showing a loss of Nissl substance and darkly eosinophilic staining cytoplasm, often irregularly bordered and shrunken in size, and by a several-layer-thick ring of mononuclear cells at their outer margins. At 6 months after low- and medium-dose SBT101 administration, histological changes were limited to minimal to moderate axonal degeneration in the cervical, thoracic, and lumbar spinal cord (Figure S7). All

Figure 5. Improved grip strength in *Abcd1⁻/y/Abcd2⁻/⁻* DKO mice after SBT101 administration

Four-paw grip strength in *Abcd1⁻/y/Abcd2⁻/⁻* DKO mice at 15 months of age. *$p < 0.05$. Data represent mean ± 95% confidence interval.

DISCUSSION

SBT101 is a nonreplicating recombinant AAV9 gene therapy vector containing a cDNA copy of the functional h*ABCD1* gene. In the series of mouse-based preclinical *in vitro* and *in vivo* analyses, SBT101 was efficacious in cells and compartments affected in AMN and partially correcting the biochemical defects underlying AMN. In hemizygous *Abcd1⁻/y* mice and *Abcd1⁻/y/Abcd2⁻/⁻* DKO mice, a single intrathecal dose of SBT101 was sufficient to increase hABCD1 expression and mtDNA levels in the spinal cord, and to reduce VLCFA levels. Indeed, previous work has shown that VLCFA accumulation, as a result of ABCD1 peroxisomal membrane transporter loss of function in AMN, leads to oxidative stress, impaired mitochondrial metabolism, and neurodegeneration.[3,7,8,26] In DKO mice, levels of the inflammatory cytokine TNF-α approached normal levels with SBT101 treatment and mice demonstrated greater grip strength relative to control animals. The observed improved grip strength was not dose dependent because the prevention of loss of grip strength was observed at the lowest dose. This may have occurred because SBT101 was administered prior to the onset of symptoms.

Functional improvements detected in DKO mice demonstrate the validity of lumbar spinal cord administration. Other injection sites in mouse models of AMN, such as brain cisterna magna, may impact the outcomes of SBT101 therapy. Because the axonal degeneration occurring in *Abcd1⁻/y* and DKO mice appears to be of a dying-back pathology,[27,28] reaching the body of the cortical motor neuron may be necessary to prevent or mitigate disease progression. However, recent studies suggest low expression of ABCD1 in mouse and human motor cortical motor neurons.[29] Improvements observed in DKO mice are particularly encouraging compared with single-knockout mice, because DKO mice exhibit earlier onset and more severe disease, likely due to their impaired ability of ABCD2 overexpression to compensate for ABCD1 deficiency.[25] Indeed, ABCD2 is differentially expressed compared with ABCD1, with higher expression in astrocytes, which have an integral role in axon development, function, and repair, and synapse connectivity.[30–32]

The current investigations with SBT101 follow two earlier preclinical studies that also showed potential benefits of an AAV9-*ABCD1* gene therapy in mouse models of AMN.[15,16] Using an AAV9 vector, the first *in vitro* study showed efficient delivery of *ABCD1* to *in vitro* cultures of primary mixed brain glial cells from *Abcd1*-Null mice and fibroblasts from patients with AMN, with dose-dependent reductions in VLCFA levels.[15] VLCFA was also decreased in the brains and spinal cords of *Abcd1⁻/y* mice following AAV9-*ABCD1* administration to the CNS via stereotactic intracerebroventricular or intravenous injections.[15] In addition, the mouse study demonstrated that AAV9-mediated *ABCD1* gene transfer was able to reach target cells in the CNS and adrenal gland. In the second mouse study, intrathecal administration of AAV9-h*ABCD1* in *Abcd1⁻/y* mice led to biochemical correction of VLCFA levels within the spinal cord and DRG, with a reduction of 17% when using osmotic pump delivery and 15% when using bolus injection.[16] Overall, these analyses demonstrated widespread delivery of recombinant AAV9 to the spinal cord, yielding rapid and robust transgene expression and reductions in VLCFA levels, findings that were further supported by the present studies.

Broadly, there was good agreement between the 8-week mouse dose-finding study and the DKO mouse study regarding the minimum dose required to produce both reductions in VLCFA levels and functional improvements in grip strength. The current work also identified a minimum effective dose for SBT101 in mice (considered to be 2.0E10 vg/an) based on doses that resulted in significant changes in biochemical markers of ABCD1 activity, including effects on mitochondrial DNA levels. Together with the doses assessed in studies of SBT101 in NHPs, the data were used to inform suitable test doses for the PROPEL trial (ClinicalTrials.gov identifier NCT05394064), the first-in-human study.

The NHP studies reported here evaluated the biodistribution of the AAV9 viral vector (using a GFP reporter gene) and the toxicology of SBT101, a gene therapy candidate for AMN, in male cynomolgus macaques. Analyses of this type are an important segue between preclinical murine models and clinical trials in human patients for developing therapies. The biodistribution studies in NHPs described here evaluated administration routes and infusion parameters, building on
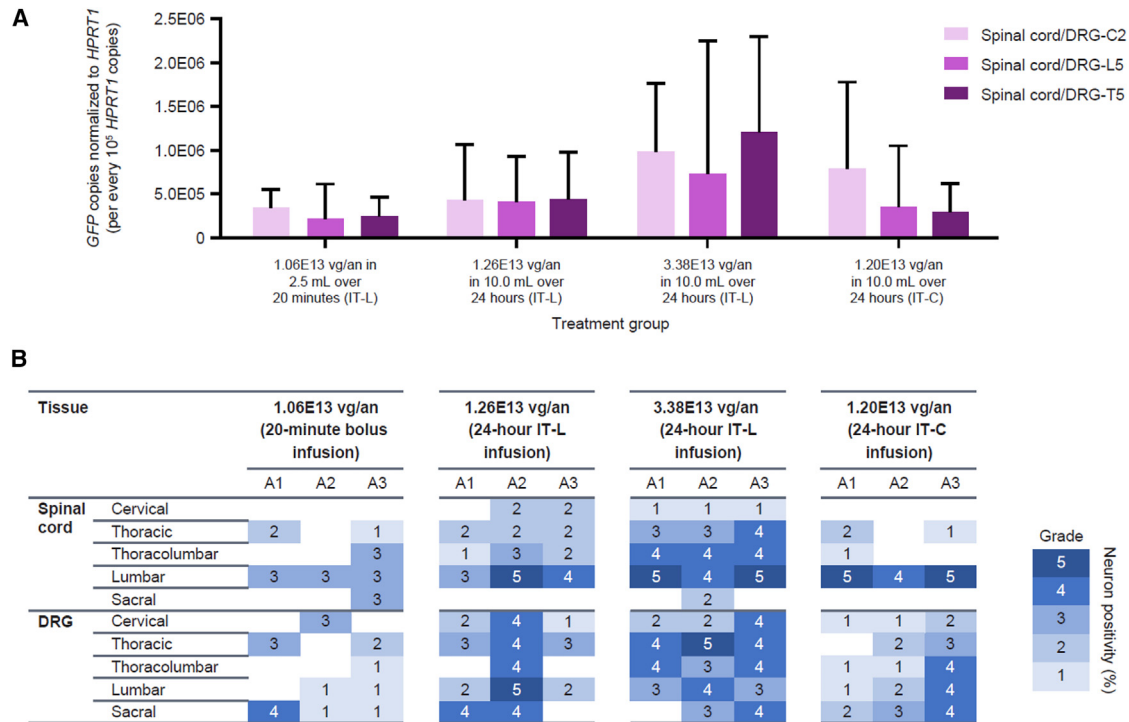
Figure 6. Vector genome biodistribution in the spinal cord and DRG according to delivery method in NHP study 1
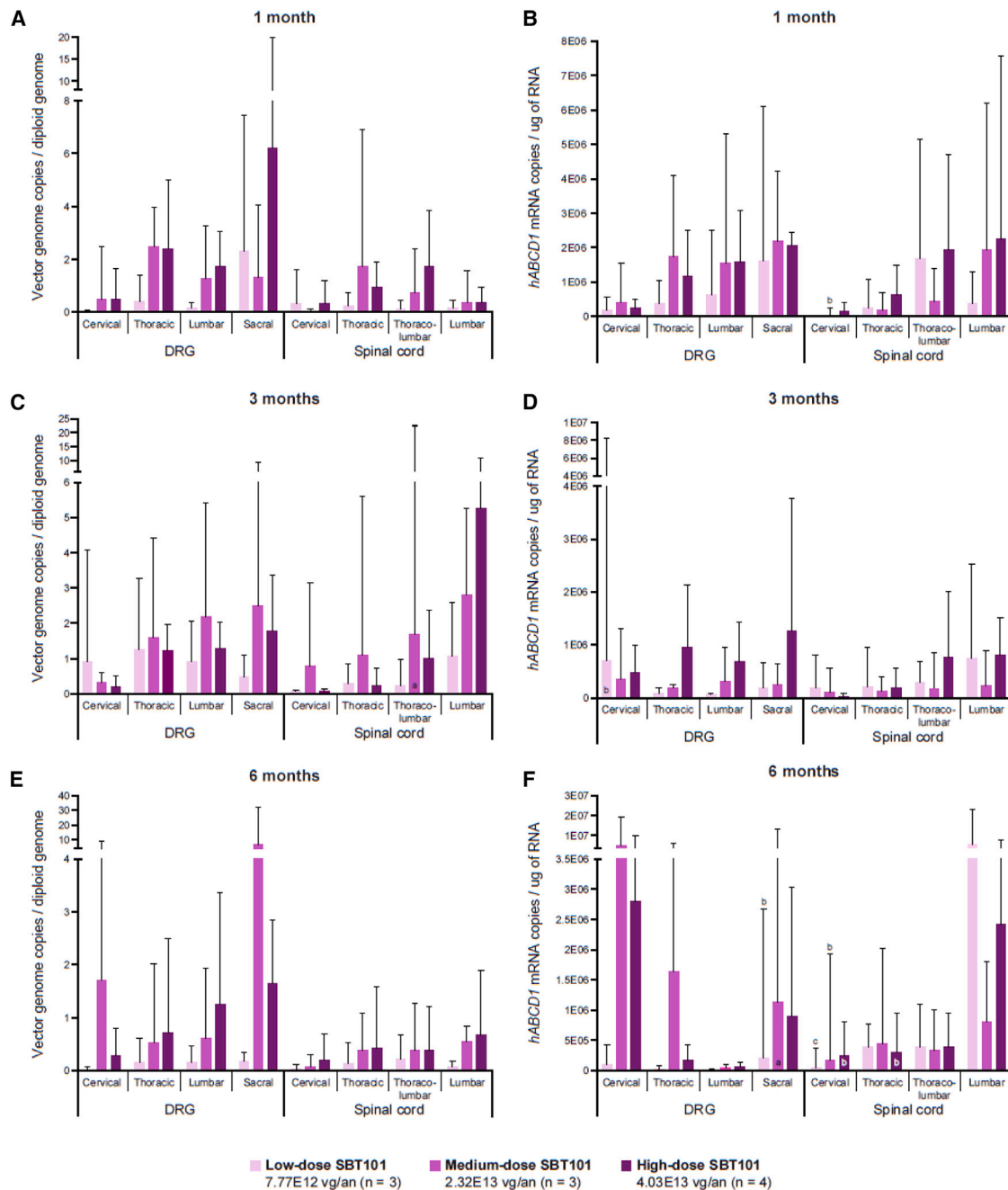
Vector genome biodistribution in the spinal cord and DRG was assessed via ddPCR quantification of GFP copies (A) and via immunohistochemical quantification of neuron positivity (B). Plotted values represent mean ± 95% confidence interval. $n = 3$ NHPs per treatment group, and A1–A3 represent individual NHPs. Percentage neuron positivity is presented as grades 1–5: grade 1, <1%; grade 2, 1%–25%; grade 3, 26%–50%; grade 4, 51%–75%; grade 5, 76%–100%; blanks, unremarkable (no observable GFP immunoreactivity). C2, cervical section 2; ddPCR, droplet digital PCR; DRG, dorsal root ganglia; GFP, green fluorescent protein; *HPRT1*, hypoxanthine-guanine phosphoribosyltransferase 1; IT-C, intrathecal cervical; IT-L, intrathecal lumbar; L5, lumbar section 5; T5, thoracic section 5; vg/an, vector genomes/animal.

two proof-of-concept studies in mice.[15,16] The first NHP study (NHP study 1) demonstrated that administration of the AAV9 vector as a 24-h infusion was associated with greater vector genome and transgene biodistribution across the lumbar, thoracic, and cervical regions of the spinal cord and DRG than a 20-min bolus delivery. Extended infusion times have not previously been reported in publications; this is a relatively simple method of delivery that increased biodistribution in particular to the cervical spinal cord. The extended time of delivery is thought to permit further delivery through CSF flow and may boost treatment efficacy due to increased coverage of the spinal cord. The second NHP study (NHP study 2) subsequently demonstrated that reductions in infusion time (24 to 6 h) and volume did not negatively affect vector genome biodistribution. Shorter infusion time and lower infusion volume increase the clinical feasibility of the administration procedure. Quantification of neuron positivity identified GFP expression in 25%–100% of cells across the spinal cord and DRG (Figure 6B). This level of transduction is within the predicted therapeutic range of approximately 23% of neurons. This was based on previous findings showing that, owing to random X-inactivation, 23%–86% of fibroblasts and white blood cells carrying the pathogenic *ABCD1* variant lacked ABCD1 expression in asymptomatic women.[33,34]

Safety assessments showed that SBT101 was well tolerated in NHPs, with no SBT101-related mortality or clinical signs recorded following single infusions at varying doses. Observations within the DRG, spinal cord, and peripheral nerves were generally consistent with those described following administration of AAV9 or similar viruses.[35,36] There were no significant differences in safety findings in neurologic tissues between treated and control animals and no dose-related toxicities. Changes in serum chemistry (ALT and AST levels) indicated a negative but transient hepatocellular response to SBT101 administration that resolved over time. Similar responses in transaminase activity have been reported with other AAV9 therapies.[37,38]

The apparent absence of DRG pathology observed with SBT101 may at first appear to be inconsistent with a 2020 meta-analysis of data from 237 rhesus macaques and 19 cynomolgus macaques in 33 studies.[36] The meta-analysis reported that DRG pathology was present in 83% of animals treated with AAV via the CSF (based on data covering five different capsids, five different promoters, and 20 different transgenes), and it was therefore considered to be a universal adverse event of AAV administration. However, the DRG pathology reported in the meta-analysis ranged from minimal to moderate in most animals and became less severe after 6 months.[36] This is indeed

Figure 7. Vector genome biodistribution and h*ABCD1* mRNA expression

Vector genome biodistribution (A, C, and E) and h*ABCD1* mRNA expression (B, D, and F) in NHP target tissues at 1 month (A and B), 3 months (C and D), and 6 months (E and F) post SBT101 administration in NHP study 4. Data represent mean ± 95% confidence interval. Vector genome copies and h*ABCD1* mRNA expression were below the limit of detection (LOD) for almost all controls (*n* = 3; data not plotted). Control NHPs received vehicle control (poloxamer [Kolliphor P188], potassium chloride, potassium di-hydrogen phosphate dibasic in sterile water). [a]One NHP did not have a calculated measurement. [b]One NHP had a measurement below the limit of quantification. [c]One NHP had a measurement below the LOD. Vector genome biodistribution and h*ABCD1* mRNA expression in NHP study 3 and NHP study 5 are shown in Figures S9 and S10, respectively. Vector genome biodistribution and h*ABCD1* mRNA expression in other tissues are shown in Figures S11–S13. DRG, dorsal root ganglia; h*ABCD1* human adenosine triphosphate-binding cassette sub-family D member 1; mRNA, messenger RNA; vg/an, vector genomes/animal.
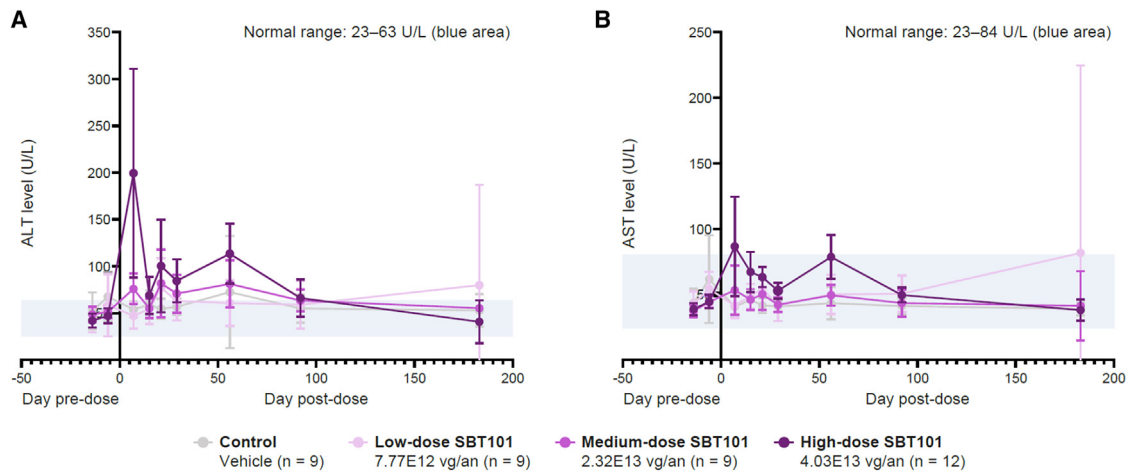
Figure 8. ALT and AST levels post SBT101 administration in NHP study 4

ALT and AST activity were assessed in samples collected before and after a 6-h lumbar infusion of SBT101. (A and B) show samples collected before SBT101 administration on days −14 and −6, and after administration on days 7, 15, 21, 29, 56, 93, and 183. Data represent mean ± 95% confidence interval. Blue shaded areas indicate normal ranges for ALT and AST levels. Control NHPs received vehicle control (poloxamer [Kolliphor P188], potassium chloride, potassium dihydrogen phosphate dibasic in sterile water). (A and B) Data at day 56 and day 93 were based on n = 6 for controls and both low- and medium-dose SBT101 and n = 8 for high-dose SBT101; data at day 183 were based on n = 3 for controls and both low- and medium-dose SBT101 and n = 4 for high-dose SBT101. ALT and AST levels in NHP study 3 and NHP study 5 are shown in Figures S14 and S15, respectively. ALT, alanine aminotransferase; AST, aspartate aminotransferase; vg/an, vector genomes/animal.

consistent with our findings, which showed minimal to moderate DRG pathology at 1 to 3 months that was largely resolved by 6 months and fully resolved by 12 months, with no associated clinical findings.

Our NHP studies show that the AAV9 vector containing a GFP reporter gene could be widely distributed throughout the CNS of NHPs following intrathecal administration, with GFP expression in 25%–100% of spinal cord and DRG neurons. Effective distribution supports the continued use of SBT101, an AAV-mediated gene therapy delivering a functional copy of the h*ABCD1* gene, as a potential treatment for AMN. The NHP biodistribution and safety studies showed that SBT101 was well tolerated over 12 months with persistent distribution of vector genomes and expression of ABCD1 mRNA in healthy NHPs without drug-related effects on clinical, ophthalmological, neurobehavioral, or cardiac observations. The extensive biodistribution and persistence of intrathecally administered SBT101 observed in our studies builds on previous literature that positions the AAV9 vector as an effective platform for gene therapy delivery. The transient safety signals observed in these studies showed that an AAV9-based approach to gene therapy is well tolerated in NHPs. Indeed, there were no significant differences in safety findings in neurologic tissues between treated and control animals, and no dose-related toxicities.

In summary, SBT101 is an AAV-mediated gene therapy candidate that efficiently delivers a functional copy of the h*ABCD1* gene to appropriate target tissues. In mouse models of human AMN, SBT101 reduced biochemical and functional signs of disease. Given the current lack of disease-modifying therapies for this disease, the development of novel strategies with impacts on biochemical and functional defects remains a key priority. SBT101 offers the potential to address the cause of this disease by restoring expression of the hABCD1 protein within spinal cord and DRG cells, thereby possibly halting disease progression and/or leading to improvements in neurological pathology. These preclinical analyses have been used to inform doses for selected SBT101 delivery in humans that are predicted to be clinically relevant in patients with AMN. The phase 1/2 PROPEL trial (ClinicalTrials.gov identifier NCT05394064) in patients with AMN is ongoing and will assess the safety and efficacy of SBT101 at different doses in humans.

MATERIAL AND METHODS

Study designs for mouse studies

In an *in vitro* analysis, mixed glial cell cultures from *Abcd1*-Null mice were used to evaluate the effects of different doses of SBT101 (Vector BioLabs, Malvern, PA, USA; multiplicity of infection [MOI]: 3.3E4, 1.0E5, or 3.3E5 vg/cell) or control solution PBS. SBT101 comprised an AAV9 vector carrying a functional copy of h*ABCD1* under the control of a cytomegalovirus enhancer/chicken β-actin promoter.

Three separate *in vivo* mouse studies were performed with each one assessing a single-dose intrathecal injection of SBT101. The first was an 8-week, dose-finding, proof-of-concept mouse study in hemizygous *Abcd1* knockout male mice (*Abcd1*$^{-/y}$; these have a phenotype mimicking features of human AMN at older age),[28] receiving one of three different doses of SBT101 (2.0E9, 6.0E9, or 2.0E10 vg/an) or control treatment (formulation buffer). In the second mouse study, *Abcd1*$^{-/y}$ mice received SBT101 at 5.5E10, 1.6E11, or 5.5E11 vg/an, or control (formulation buffer) and were followed for 13 or 24 weeks. In the third mouse study, *Abcd1*$^{-/y}$/*Abcd2*$^{-/-}$ DKO

mice were used. This model presents more pronounced signs of disease earlier in life, because the ABCD2 transporter shares overlapping biochemical function with ABCD1.[26] DKO mice received SBT101 at doses of 3.3E10 or 3.3E11 vg/an, or control (AAV9-Null vector at 1.6E11 vg/an) and were followed for up to 11 months. WT mice were included in all three studies and received only control treatments.

Study designs for NHP studies

Five individual studies in male cynomolgus macaques were conducted. NHP studies 1 and 2 assessed the biodistribution of intrathecally administered AAV9 vector containing the DNA sequence for a GFP reporter gene. The AAV9 vector was chosen because it is the established gold standard for vector-mediated gene therapy in CNS disorders.[39] In NHP study 1, animals received treatment as a 20-min bolus delivery in the lumbar region (1.06E13 vg/an), a 24-h lumbar infusion (1.26E13 or 3.38E13 vg/an), or a 24-h cervical infusion (1.20E13 vg/an). One control animal did not receive a catheter and was untreated. In NHP study 2, animals received a single administration (target dose, 3.25E13 vg/an) via lumbar infusion but with differing infusion durations (6 or 24 h) or dosing volumes (2.5–10 mL); control animals were untreated (with or without a catheter). Animals were sacrificed on day 15 post administration in both biodistribution studies.

NHP studies 3 to 5 were safety analyses assessing the safety of SBT101 (NHP studies 3 and 4, Brammer Bio, Alachua, FL, USA; NHP study 5, Yposkesi, Corbeil-Essonnes, France) in male cynomolgus macaques receiving a single 6-h, intrathecal lumbar infusion of SBT101 (doses ranged from 7.77E12 to 7.62E13 vg/an) or vehicle control. Animals were followed for 1 month (NHP study 4), 3 months (NHP studies 3 and 4), 6 months (NHP studies 3 and 4), and 12 months (NHP study 5) post SBT101 administration. Equal numbers of animals were sacrificed per scheduled time point in the respective studies. However, all animals receiving SBT101 at 7.62E13 vg/an in NHP study 3 were only followed for 3 months.

Treatments for mouse studies

Mixed glial cells were passaged onto six-well plates (2.0E5 cells/well) for 24 h and transduced with varying MOIs of SBT101 for 5 days. Briefly, 1- to 2-day old *Abcd1*-Null and WT pups were euthanized, their brains dissected, and the hindbrains removed. After washing twice with PBS, brain tissue was incubated with 0.05% trypsin for 10 min followed by 5-min incubation in DNaseI. Digested brain tissues were disaggregated using a 10-mL pipette and passed over a 40-μm filter. Filtered cells were collected by centrifugation, suspended in Dulbecco's modified Eagle's medium containing 10% fetal bovine serum, and cultured at 37°C until confluent.

For the three *in vivo* analyses, mice received a single intrathecal dose of SBT101 or control treatment. Dosing solutions were prepared on the day of dosing. Test material was thawed and diluted to the appropriate concentration and volume in formulation buffer (0.001% Pluronic F-68 in 1× PBS). Animals were anesthetized

with isoflurane; the levels of anesthetics were adjusted for each animal by monitoring respiration before the surgical procedure. After the skin over the lumbar region was shaved and cleaned, a 2- to 3-cm mid-sagittal incision was made through the skin, exposing the muscle, and left epaxial muscles at lumbar region were separated from vertebrae. Dose volume was 10 μL per animal administered slowly delivered using a Hamilton syringe (Sigma-Aldrich, St. Louis, MO, USA) by manual injection to the lumbar spine at the L3–L4, L4–L5, or L5–L6 intravertebral spaces, as previously described.[40] The needle was placed longitudinally to the spine, with the tip directed to the cranial part, and was carefully introduced into the foramen around 4–5 mm. The proper position of the needle was confirmed by a tail flick reflex. The needle was removed 15 s after finishing vector delivery to favor spread through the CSF and avoid reflux to the periphery.

Two of the *in vivo* mouse studies used the original SBT101 vector known as SBT101.V1; the third mouse study (as well as the *in vitro* study) used a more stable version that was developed later, known as SBT101.V3. There are no differences between SBT101.V1 and SBT101.V3 in the expression cassette; the only differences are in the plasmid backbone and immediately adjacent to the inverted terminal repeat sequence. Both versions carry the same promoter, transgene (h*ABCD1*), and poly(A) signal sequences.

Treatments for NHP studies

Animals received single intrathecal doses of either the AAV9 vector with the GFP reporter gene (NHP biodistribution studies 1 and 2) or SBT101 (NHP safety studies 3, 4, and 5). The AAV9 vector contained the DNA sequence for the GFP reporter gene, a cytomegalovirus enhancer-chicken β-actin (CBA) promoter to drive expression, and the woodchuck hepatitis virus post transcriptional regulatory element (WPRE) to enhance transgene expression. AAV9-CBA-GFP-WPRE was diluted in 0.001% Pluronic-F68 in Dulbecco's PBS (without calcium and magnesium; formulation buffer). SBT101 was diluted in vehicle control (0.001% poloxamer [Kolliphor P188], potassium chloride, potassium dihydrogen phosphate dibasic in sterile water), and supplied in ready-to-use vials.

Treatment was administered via a catheter implanted at the L4, L5, or L6 vertebra for lumbar delivery or the C2 vertebra for cervical delivery. A calibrated syringe infusion pump was used for 20-min bolus delivery at the lumbar region, and a calibrated ambulatory pump was used to deliver 24-h infusions at the lumbar and cervical regions or 6-h lumbar infusions.

Animals for mouse studies

WT C57BL/6J mice were obtained either from Charles River Laboratories (Hollister, CA, USA) or from the study sponsor's colony, and *Abcd1*[−/y] mice were obtained from the study sponsor's colony.[15] DKO mice were sourced from the animal breeding facility of IDIBELL (Barcelona, Spain). Primary brain glial cell mixed cultures were derived from WT and *Abcd1*-Null C57BL/6J mice, as described above.

Animals were housed in conventional housing (clear polycarbonate cages), fed a standard diet, and maintained under a 12-h light-dark cycle. All mice were weighed before treatment and at least weekly thereafter. Cage-side health checks were performed at least daily. Animals were checked for morbidity, mortality, and moribundity. Clinical observations were made on a similar time frame to health checks. Mice also underwent routine behavioral testing, including one or more of the following assessments: grip strength, mechanical allodynia, clasping, balance beam, bar cross, and treadmill.

Mice were euthanized at study end or if determined moribund. Animals were sacrificed via anesthetization and perfusion with 4% paraformaldehyde.

Animals for NHP studies
Male cynomolgus macaques (*Macaca fascicularis*) were obtained from Alpha Genesis (Yemassee, SC, USA) for NHP studies 1 and 2, from Worldwide Primates (Miami, FL, USA) for NHP study 3, and Envigo Global Services (Alice, , USA) in NHP studies 4 and 5.

Animals were housed in conventional housing (steel cages), fed a standard diet, and maintained under a 12-h light-dark cycle; they were provided with environmental enrichment.

All animals were weighed before treatment and at least weekly thereafter. Cage-side health checks were performed at least twice daily. Animals were checked for morbidity, mortality, and moribundity. Clinical observations were conducted on a similar time frame to health checks. Cynomolgus macaques receiving AAV9-CBA-GFP-WPRE underwent a battery of clinical pathological tests, and those receiving SBT101 underwent cardiac, neurobehavioral, ophthalmic, and physical examinations, with vital signs also recorded.

All NHPs were sacrificed at study end or euthanized if determined moribund (with the approval of the veterinarian, study director, and/or sponsor representative). Animals were sacrificed through anesthetization and exsanguination.

Sample collection and assessments for mouse studies
In the *in vivo* mouse studies, spinal cord was collected at terminal euthanasia of mice, and the DRG were also collected in the DKO mouse study. Assessments conducted in each of the studies are described in more detail below. A range of tissues were collected from all mice in each study, but only analyses of spinal cord and DRG are described here.

Sample collection and assessments for NHP studies
Samples of CSF and blood were collected at scheduled intervals wherever possible, and at terminal sacrifice. Necropsy was performed on all animals at terminal sacrifice and tissues were collected from several organs, including DRG, spinal cord, kidney, liver, heart, and skeletal muscle. Assessments performed in each of the five NHP studies are described in more detail below; a summary of NHP studies can be found in Table S1.

hABCD1 protein expression for mouse studies
The expression of hABCD1 was assessed using the same approach in both *in vitro* and *in vivo* samples. Tissues were homogenized with a steel bead in water containing $1\times$ protease inhibitor cocktail (6 µL/mg tissue) using a TissueLyser II homogenizer (QIAGEN, Germantown, MD, USA). Following homogenization, the pellet was collected by centrifugation, and the supernatant was discarded. Pellets were resuspended in solubilization buffer (2% NP40, 2% sodium deoxycholate, 0.2% sodium dodecyl sulfate, 5 mM EDTA, and $1\times$ protease inhibitor cocktail in $1\times$ PBS) and insoluble proteins were removed by centrifugation. Extracted proteins were quantified by capillary electrophoresis-based immunodetection using 0.0025–0.25 µg/µL of total protein (Jess, ProteinSimple, San Jose, CA, USA) with an anti-hABCD1 antibody (Origene Laboratories, Rockville, MD, USA). A four-point (*in vitro* study) or 10-point (*in vivo* studies) standard curve using recombinant hABCD1 was employed to determine hABCD1 levels. Human recombinant ABCD1 (80 ng/µL; obtained from Origene Laboratories) was used as a positive control. hABCD1 expression was estimated by interpolating Jess signal peak areas of samples with signal peak areas of known concentration of the recombinant hABCD1 protein standard.

Total VLCFA and C26:0-lysophophatidylcholine levels
To assess the effect of SBT101 on C22:0, C24:0, C26:0, and C26:0-lysophosphatidylcholine (LPC) levels in mixed glial cell cultures, extracts were prepared by homogenizing the cell culture pellets directly in water, followed by acid hydrolysis, alkaline hydrolysis, and extraction in hexane. Fatty acids were analyzed from the cell culture extracts on a gas chromatography mass spectrometer (Hewlett-Packard 5890/5973, Palo Alto, CA, USA) equipped with a CPsil 5 low-bleed capillary column (Chrompack 25 m $\times$ 0.25 mm internal diameter [ID], film thickness 0.25 µm). For separation, the temperature was initiated at 60°C (held for 1 min), increased to 160°C at 30°C/min, then increased to 230°C at 5°C/min, and subsequently to 320°C at 20°C/min and held for 10 min. The injection and interface temperature were 300°C. The injection volume was 1 µL at splitless mode with a splitless time of 1.5 min. Helium was used as the carrier gas (50 kPa). Electron impact ionization was applied at 70 eV.

In the *in vivo* mouse studies, levels of C26:0-LPC were measured in spinal cord tissue from mice treated with SBT101 or control by high-performance liquid chromatography with tandem mass spectrometry as described previously.[41]

Viral genomes and mtDNA copy numbers for mouse studies
Viral genomes copy number was measured in genomic DNA extracted from mouse tissues that had been homogenized in water containing $1\times$ protease inhibitor cocktail (a method developed to produce tissue homogenates that were compatible with VLCFA, protein, and DNA analyses). In *in vivo* mouse studies 1 and 2 the absolute number of viral genomes was assessed by droplet digital polymerase chain reaction (ddPCR) in relation to an endogenous nuclear gene, *RPP30*. To determine the concentration of target DNA, the QuantaSoft Analysis software (Bio-Rad, Hercules, CA, USA) was

used to fit the positive droplets to a Poisson distribution. Absolute quantification of mtDNA copy numbers in mouse spinal cord tissue was also evaluated via the same ddPCR approach using *ND1* (a gene present on the mitochondrial genome) in relation to *RPP30*.

In the DKO mouse study, viral genome copy number was measured in mouse tissues processed by a QIAmp DNA Mini Kit (QIAGEN) and followed by quantitative real-time PCR. Viral genome copy number per cell was calculated using primers for cyclophilin B as the reference gene, or SBT101 or AAV9-Null constructs with the forward and reverse primers targeting the SV40 polyadenylation sequence (forward primer, 5′-CGCTCTAGAAAGAGATCCAGACATG-3′; reverse primer, 5′-TTTCACTGCATTCTAGTTGTGGTTT-3′; probe, 5′-FAM-AAGATACATTGATGAGTTTGG/MGB/NFQ-3′). Viral genome copy numbers per cell were calculated using a standard curve generated from known amounts of a plasmid DNA containing the SBT101 sequence or a 525-base-pair cyclophilin B PCR product (forward, 5′-CATGCCTATG GTCCTAGCTT-3′; reverse, 5′-GGTTTCTCCACTTCGATCTTGC-3′) purified by Geneclean (MP Biomedicals, Santa Ana, USA) in 10 ng/mL of salmon sperm DNA. Calculations assumed that 1 mg of mouse genomic DNA contained 1.33E8 diploid genomes.

Vector genome biodistribution for NHP studies
In the two NHP biodistribution studies, vector genome biodistribution in the spinal cord and DRG was assessed using droplet digital PCR (ddPCR) quantification of GFP copies. Spinal cord and DRG tissue samples were placed into clean tubes, frozen on dry ice, and stored at −60°C. Sample testing was conducted by Precision for Medicine (Houston, TX, USA) according to a validated ddPCR-based duplex assay for the quantification of AAV9-GFP vector from animal tissues using the QX200 ddPCR system (Bio-Rad, Hercules, CA, USA). This assay targeted the GFP transgene on the vector genome, and a single-copy gene (hypoxanthine-guanine phosphoribosyltransferase 1 [*HPRT1*]) on the cynomolgus macaque genome, enabling simultaneous quantification of vector genome copies and copies of the host animal cell genome. Copy numbers of GFP were normalized to *HPRT1*.

In the NHP safety studies, biodistribution was evaluated using qPCR for the presence of vector genomes (reported as the number of vector DNA copies/μg genomic DNA in NHP study 3 and vector DNA copies/diploid genome in NHP studies 4 and 5) using a validated method.

hABCD1 mRNA analysis for mouse studies
In the DKO mouse study, frozen tissue sections in stabilization buffer (RNAlater, Thermo Fisher Scientific, Waltham, MA) extracted using the RNeasy Kit (QIAGEN) were analyzed by RT-PCR to assess the relative mRNA level for *ABCD1*.

hABCD1 mRNA analysis for NHP studies
Collected during the NHP safety studies, frozen tissue samples in stabilization buffer (RNAlater, Thermo Fisher Scientific, Waltham, MA) were analyzed by RT-PCR for the relative mRNA expression level of *ABCD1* using a validated method (Labcorp Drug Development Laboratories, IN, USA).

Immunohistochemistry for mouse studies
In the DKO mouse study, thoracic spinal cord and DRG were cryoprotected with 30% sucrose and embedded in Tissue-Tek OCT compound (Sakura, Alphen aan den Rijn, the Netherlands). Sections (10 μm thick) were permeabilized with methanol and washed with blocking buffer (0.05 M Tris + 0.3% Triton X-100 + 3% bovine serum albumin + 5% fetal bovine serum) for 1 h. Tissue sections were incubated in primary antibodies overnight at 4°C and secondary antibodies for 1 h. Spinal cord was labeled with primary antibodies against glial fibrillary acidic protein (dilution 1/800 [Invitrogen, Waltham, MA, USA, 2.2B10 130300]), hABCD1 (1/500 [Abcam, Waltham, MA, USA, ab197013]), and neuronal nuclei (NeuN; 1/100 [Merck, Burlington, MA, USA, clone A60 MAB 377]). DRG sections were labeled with primary antibodies against hABCD1 and protein gene product 9.5 (1/500 [Invitrogen, A21200]). Labeled sections were subsequently fluorescently tagged with secondary antibodies conjugated with Alexa Fluor 488 (green) or 647 (magenta) (Invitrogen, A11085 and A21247, respectively) or Cy3 (red) (Jackson ImmunoResearch, West Grove, PA, USA, 711-165-152) and counterstained with Hoechst 33258 stain (blue) (Sigma, H6024). Fluorescently labeled slides were analyzed by confocal microscopy (ZEISS LSM 700) and quantified using ImageJ software.

GFP immunohistochemistry for NHP studies
Effective transduction with the vector was assessed by immunohistochemical quantification of GFP positivity within neurons. Spinal cord and DRG tissues were fixed in 10% neutral-buffered formalin at ambient temperature. After 48 h (±4 h), samples were transferred to PBS and stored at 1°C–8°C before shipment to Tox Path Specialists (Frederick, MD, USA) for processing and analysis. Briefly, tissues were embedded in paraffin and sectioned using a 5-μm block advance. Spinal cord sections (cervical, thoracic, lumbar, and sacral) were cut in transverse and oblique sections, and spinal cord sections from the catheter tip (treatment site) were cut in multiple transverse sections. Immunoreactivity to GFP was assessed on serial sections using brightfield microscopy (negative isotype was used for serial control sections). Cell type was based on morphological analysis, and neurons were identified. The proportion of neurons with positive GFP labeling was calculated and graded as follows: grade 1, <1%; grade 2, 1%–25%; grade 3, 26%–50%; grade 4, 51%–75%; and grade 5, 76%–100%.

TNF-α levels for mouse studies
Levels of TNF-α were measured using RT-PCR, as previously described.[42] Briefly, TNF-α expression was analyzed using TaqMan Gene Expression Assays (Thermo Fisher Scientific, Waltham, MA, USA) and standardized TaqMan probes on a LightCycler 480 Real-Time PCR System (Roche Diagnostics, Barcelona, Spain). Relative quantification was carried out using the Delta-Delta Ct (ΔΔCt) method with ribosomal protein lateral stalk subunit P0 (*RPLP0*) RNA as the reference.

Grip strength for mouse studies

Grip strength was assessed only in the DKO mouse study. To test forelimb and hindlimb grip strength, animals were placed over a metallic grid and the four paws allowed to grasp the bars while being gently pulled away by the tail, parallel to the grid. During the test, the instrument (Ugo Basile Grip Strength Meter; Varese, Italy) recorded the peak pull force prior to release of the mouse from the grid. Each animal was tested at least three times and was allowed to rest between each trial, after which the apparatus was cleaned with ethanol. The maximum force exerted was recorded in grams.

Neutralizing antibodies for NHP studies

Serum and CSF samples were analyzed for NAbs to AAV9 by Gene Therapy Program (Translational Research Labs, University of Pennsylvania, PA, USA).[43]

Serum chemistry for NHP studies

Levels of ALT and AST activity were assessed as part of routine clinical chemistry.

Histopathology for NHP studies

DRG, spinal cord, and various peripheral tissues (e.g., heart, kidney, muscle, and liver) were fixed in 10% neutral-buffered formalin and embedded in paraffin. Blocks were sectioned at a nominal thickness of 5 μm and stained with hematoxylin and eosin. Stained sections were examined microscopically by the principal investigator for anatomic pathology. Axon degeneration, mononuclear cell infiltrate, and neuron necrosis were graded 0–5 as follows: grade 0, unremarkable; grade 1, minimal; grade 2, slight; grade 3, moderate; grade 4, marked; and grade 5, severe.

Ethics

All methods employed in these mouse studies were in accordance with the ARRIVE (Animal Research: Reporting of In Vivo Experiments) guidelines, the Guide for the Care and Use of Laboratory Animals (Guide, eighth edition, 2011, National Institutes of Health), and European (2010/63/EU) and Spanish (RD 53/2013) legislation. Experimental protocols were approved by IDIBELL, Institutional Animal Care and Use Committee, and regional authority (DMAH 11032). Studies were conducted in accordance with the standard operating procedures of the testing facilities and relevant site regulations and complied with all applicable sections of one or more of the following: the Final Rules of the Animal Welfare Act Regulations (Title 9, Code of Federal Regulations); the Guide for the Care and Use of Laboratory Animals, Institute of Laboratory Animal Resources, Commission on Life Sciences, National Research Council, eighth edition; the Public Health Service Policy on Humane Care and Use of Laboratory Animals; and Biomere's Institutional Animal Care and Use Committee and animal care and use policies.

Testing facilities for mouse studies, including the IDIBELL animal facility (Unit 1155), were fully accredited by the Association for Assessment and Accreditation of Laboratory Animal Care. Any research that involved recombinant DNA as well as all materials that may have biosafety concerns is reviewed and approved by the testing facilities Institutional Biosafety Committee. Through daily routine monitoring, any signs of discomfort or distress are reported, and appropriate measures are taken by veterinary staff to treat and relieve animal distress or, if necessary, to treat or euthanize animals.

All NHP studies were conducted in accordance with the standard operating procedures of the testing facilities and relevant site regulations. NHP studies 1 and 2 complied with all applicable sections of the following: the Final Rules of the Animal Welfare Act Regulations (Title 9, Code of Federal Regulations) and the Guide for the Care and Use of Laboratory Animals, Institute of Laboratory Animal Resources, Commission on Life Sciences, National Research Council, eighth edition. NHP studies 3–5 complied with all applicable sections of the following: the Final Rules of the Animal Welfare Act Regulations (Title 9, Code of Federal Regulations); the Guide for the Care and Use of Laboratory Animals; and the Office of Laboratory Animal Welfare, National Institutes of Health. All efforts were made to minimize animal suffering. All NHP studies were approved by the ethics committees of their respective contract research organizations.

Statistical analysis

Results are expressed as mean and 95% confidence interval; relevant results were analyzed for statistical significance by one-way analysis of variance (ANOVA) followed by Dunnett's post-test. For biodistribution studies in cynomolgus macaques, only descriptive statistics are presented. No statistical analyses were performed.

DATA AND CODE AVAILABILITY

All data underpinning the findings presented in this article are available upon reasonable request from a qualified individual or institution for research purposes. For more information, please contact info@swanbioTx.com.

ACKNOWLEDGMENTS

AUTHOR CONTRIBUTIONS

All authors have made substantial contributions to the following: conceptualization, methodology, investigation, visualization, writing – original draft, and writing – review & editing. All authors have provided their final approval of the manuscript.

DECLARATION OF INTERESTS

T.L. and K.K. are employees and stock/shareholders of SwanBio Therapeutics. V.V., D.W.A., S.W.C., and H.P. were employees and stock/shareholders of SwanBio Therapeutics at the time the studies were performed: V.V. is an employee of Code Biotherapeutics; D.W.A. is an employee of Code Biotherapeutics; S.W.C. is an employee of Clithero-Clark Consulting, LLC; H.P. is an employee of Center for Breakthrough Medicines. C.A.M. has financial interests in/received consultancy fees from Chameleon Biosciences, Skylark Bio, and Sphere Gene Therapeutics; resequenceceived research support/grants from BridgeBio, SwanBio Therapeutics, and Waypoint Capital; and received royalties for licensing agreements from BridgeBio, Partners Healthcare, Skylark Bio, Sphere Gene Therapeutics, and SwanBio Therapeutics. Y.G. received royalties for licensing agreements from SwanBio Therapeutics. F.E. received research support/grants from Aspa Therapeutics, bluebird bio, Ionis Pharmaceuticals, Minoryx Therapeutics, and Sio Gene Therapies;

received consultancy fees from Autobahn Therapeutics, Poxel, SwanBio Therapeutics, Takeda, Taysha, and UpToDate; and is a founder and stock/shareholder of SwanBio Therapeutics. A.P., A.B., and S.K. received unrestricted research support/grants and consultancy fees from SwanBio Therapeutics.

SUPPLEMENTAL INFORMATION

Supplemental information can be found online at https://doi.org/10.1016/j.omtm.2024.101354.

REFERENCES

1. Kemp, S., Huffnagel, I.C., Linthorst, G.E., Wanders, R.J., and Engelen, M. (2016). Adrenoleukodystrophy - neuroendocrine pathogenesis and redefinition of natural history. Nat. Rev. Endocrinol. *12*, 606–615.

2. Zhu, J., Eichler, F., Biffi, A., Duncan, C.N., Williams, D.A., and Majzoub, J.A. (2020). The Changing Face of Adrenoleukodystrophy. Endocr. Rev. *41*, 577–593.

3. Berger, J., Forss-Petter, S., and Eichler, F.S. (2014). Pathophysiology of X-linked adrenoleukodystrophy. Biochimie *98*, 135–142.

4. Mallack, E.J., Gao, K., Engelen, M., and Kemp, S. (2022). Structure and Function of the ABCD1 Variant Database: 20 Years, 940 Pathogenic Variants, and 3400 Cases of Adrenoleukodystrophy. Cells *11*, 283.

5. Kawaguchi, K., Morita, M., and ABC Transporter Subfamily, D. (2016). Distinct Differences in Behavior between ABCD1-3 and ABCD4 in Subcellular Localization, Function, and Human Disease. BioMed Res. Int. *2016*, 6786245.

6. Morita, M., and Imanaka, T. (2012). Peroxisomal ABC transporters: structure, function and role in disease. Biochim. Biophys. Acta *1822*, 1387–1396.

7. López-Erauskin, J., Galino, J., Ruiz, M., Cuezva, J.M., Fabregat, I., Cacabelos, D., Boada, J., Martínez, J., Ferrer, I., Pamplona, R., et al. (2013). Impaired mitochondrial oxidative phosphorylation in the peroxisomal disease X-linked adrenoleukodystrophy. Hum. Mol. Genet. *22*, 3296–3305.

8. Wiesinger, C., Eichler, F.S., and Berger, J. (2015). The genetic landscape of X-linked adrenoleukodystrophy: inheritance, mutations, modifier genes, and diagnosis. Appl. Clin. Genet. *8*, 109–121.

9. Engelen, M., Kemp, S., de Visser, M., van Geel, B.M., Wanders, R.J.A., Aubourg, P., and Poll-The, B.T. (2012). X-linked adrenoleukodystrophy (X-ALD): clinical presentation and guidelines for diagnosis, follow-up and management. Orphanet J. Rare Dis. *7*, 51.

10. Kemp, S., Berger, J., and Aubourg, P. (2012). X-linked adrenoleukodystrophy: clinical, metabolic, genetic and pathophysiological aspects. Biochim. Biophys. Acta *1822*, 1465–1474.

11. Engelen, M., Barbier, M., Dijkstra, I.M.E., Schür, R., de Bie, R.M.A., Verhamme, C., Dijkgraaf, M.G.W., Aubourg, P.A., Wanders, R.J.A., van Geel, B.M., et al. (2014). X-linked adrenoleukodystrophy in women: a cross-sectional cohort study. Brain *137*, 693–706.

12. Corre, C.S., Grant, N., Sadjadi, R., Hayden, D., Becker, C., Gomery, P., and Eichler, F.S. (2021). Beyond gait and balance: urinary and bowel dysfunction in X-linked adrenoleukodystrophy. Orphanet J. Rare Dis. *16*, 14.

13. Engelen, M., van Ballegoij, W.J.C., Mallack, E.J., Van Haren, K.P., Köhler, W., Salsano, E., van Trotsenburg, A.S.P., Mochel, F., Sevin, C., Regelmann, M.O., et al. (2022). International Recommendations for the Diagnosis and Management of Patients With Adrenoleukodystrophy: A Consensus-Based Approach. Neurology *99*, 940–951.

14. Adang, L.A., Sherbini, O., Ball, L., Bloom, M., Darbari, A., Amartino, H., DiVito, D., Eichler, F., Escolar, M., Evans, S.H., et al. (2017). Revised consensus statement on the preventive and symptomatic care of patients with leukodystrophies. Mol. Genet. Metabol. *122*, 18–32.

15. Gong, Y., Mu, D., Prabhakar, S., Moser, A., Musolino, P., Ren, J., Breakefield, X.O., Maguire, C.A., and Eichler, F.S. (2015). Adenoassociated virus serotype 9-mediated gene therapy for x-linked adrenoleukodystrophy. Mol. Ther. *23*, 824–834.

16. Gong, Y., Berenson, A., Laheji, F., Gao, G., Wang, D., Ng, C., Volak, A., Kok, R., Kreouzis, V., Dijkstra, I.M., et al. (2019). Intrathecal Adeno-Associated Viral Vector-Mediated Gene Delivery for Adrenomyeloneuropathy. Hum. Gene Ther. *30*, 544–555.

17. Kaplitt, M.G., Feigin, A., Tang, C., Fitzsimons, H.L., Mattis, P., Lawlor, P.A., Bland, R.J., Young, D., Strybing, K., Eidelberg, D., and During, M.J. (2007). Safety and tolerability of gene therapy with an adeno-associated virus (AAV) borne GAD gene for Parkinson's disease: an open label, phase I trial. Lancet *369*, 2097–2105.

18. Marks, W.J., Jr., Ostrem, J.L., Verhagen, L., Starr, P.A., Larson, P.S., Bakay, R.A., Taylor, R., Cahn-Weiner, D.A., Stoessl, A.J., Olanow, C.W., and Bartus, R.T. (2008). Safety and tolerability of intraputaminal delivery of CERE-120 (adeno-associated virus serotype 2-neurturin) to patients with idiopathic Parkinson's disease: an open-label, phase I trial. Lancet Neurol. *7*, 400–408.

19. Leone, P., Shera, D., McPhee, S.W.J., Francis, J.S., Kolodny, E.H., Bilaniuk, L.T., Wang, D.J., Assadi, M., Goldfarb, O., Goldman, H.W., et al. (2012). Long-term follow-up after gene therapy for canavan disease. Sci. Transl. Med. *4*, 165ra163.

20. Worgall, S., Sondhi, D., Hackett, N.R., Kosofsky, B., Kekatpure, M.V., Neyzi, N., Dyke, J.P., Ballon, D., Heier, L., Greenwald, B.M., et al. (2008). Treatment of late infantile neuronal ceroid lipofuscinosis by CNS administration of a serotype 2 adeno-associated virus expressing CLN2 cDNA. Hum. Gene Ther. *19*, 463–474.

21. Meijer, D.H., Maguire, C.A., LeRoy, S.G., and Sena-Esteves, M. (2009). Controlling brain tumor growth by intraventricular administration of an AAV vector encoding IFN-beta. Cancer Gene Ther. *16*, 664–671.

22. Guo, Y., Wang, D., Qiao, T., Yang, C., Su, Q., Gao, G., and Xu, Z. (2016). A Single Injection of Recombinant Adeno-Associated Virus into the Lumbar Cistern Delivers Transgene Expression Throughout the Whole Spinal Cord. Mol. Neurobiol. *53*, 3235–3248.

23. Meyer, K., Ferraiuolo, L., Schmelzer, L., Braun, L., McGovern, V., Likhite, S., Michels, O., Govoni, A., Fitzgerald, J., Morales, P., et al. (2015). Improving single injection CSF delivery of AAV9-mediated gene therapy for SMA: a dose-response study in mice and nonhuman primates. Mol. Ther. *23*, 477–487.

24. Food and Drug Administration (2022). Human Gene Therapy for Neurodegenerative Diseases: Guidance for Industry (Center for Biologics Evaluation and Research).

25. Pujol, A., Ferrer, I., Camps, C., Metzger, E., Hindelang, C., Callizot, N., Ruiz, M., Pàmpols, T., Giròs, M., and Mandel, J.L. (2004). Functional overlap between ABCD1 (ALD) and ABCD2 (ALDR) transporters: a therapeutic target for X-adrenoleukodystrophy. Hum. Mol. Genet. *13*, 2997–3006.

26. López-Erauskin, J., Galino, J., Bianchi, P., Fourcade, S., Andreu, A.L., Ferrer, I., Muñoz-Pinedo, C., and Pujol, A. (2012). Oxidative stress modulates mitochondrial failure and cyclophilin D function in X-linked adrenoleukodystrophy. Brain *135*, 3584–3598.

27. Ferrer, I., Aubourg, P., and Pujol, A. (2010). General aspects and neuropathology of X-linked adrenoleukodystrophy. Brain Pathol. *20*, 817–830.

28. Pujol, A., Hindelang, C., Callizot, N., Bartsch, U., Schachner, M., and Mandel, J.L. (2002). Late onset neurological phenotype of the X-ALD gene inactivation in mice: a mouse model for adrenomyeloneuropathy. Hum. Mol. Genet. *11*, 499–505.

29. Gong, Y., Laheji, F., Berenson, A., Li, Y., Moser, A., Qian, A., Frosch, M., Sadjadi, R., Hahn, R., Maguire, C.A., and Eichler, F. (2024). Role of Basal Forebrain Neurons in Adrenomyeloneuropathy in Mice and Humans. Ann. Neurol. *95*, 442–458.

30. Hemati-Gourabi, M., Cao, T., Romprey, M.K., and Chen, M. (2022). Capacity of astrocytes to promote axon growth in the injured mammalian central nervous system. Front. Neurosci. *16*, 955598.

31. Kıray, H., Lindsay, S.L., Hosseinzadeh, S., and Barnett, S.C. (2016). The multifaceted role of astrocytes in regulating myelination. Exp. Neurol. *283*, 541–549.

32. Chung, W.-S., Allen, N.J., and Eroglu, C. (2015). Astrocytes Control Synapse Formation, Function, and Elimination. Cold Spring Harbor Perspect. Biol. *7*, a020370.

33. Feigenbaum, V., Lombard-Platet, G., Guidoux, S., Sarde, C.O., Mandel, J.L., and Aubourg, P. (1996). Mutational and protein analysis of patients and heterozygous women with X-linked adrenoleukodystrophy. Am. J. Hum. Genet. *58*, 1135–1144.

34. Watkiss, E., Webb, T., and Bundey, S. (1993). Is skewed X inactivation responsible for symptoms in female carriers for adrenoleucodystrophy? J. Med. Genet. *30*, 651–654.

35. Hinderer, C., Bell, P., Katz, N., Vite, C.H., Louboutin, J.P., Bote, E., Yu, H., Zhu, Y., Casal, M.L., Bagel, J., et al. (2018). Evaluation of intrathecal routes of administration for adeno-associated viral vectors in large animals. Hum. Gene Ther. *29*, 15–24.

36. Hordeaux, J., Buza, E.L., Dyer, C., Goode, T., Mitchell, T.W., Richman, L., Denton, N., Hinderer, C., Katz, N., Schmid, R., et al. (2020). Adeno-Associated Virus-Induced Dorsal Root Ganglion Pathology. Hum. Gene Ther. *31*, 808–818.

37. Hinderer, C., Katz, N., Buza, E.L., Dyer, C., Goode, T., Bell, P., Richman, L.K., and Wilson, J.M. (2018). Severe Toxicity in Nonhuman Primates and Piglets Following High-Dose Intravenous Administration of an Adeno-Associated Virus Vector Expressing Human SMN. Hum. Gene Ther. *29*, 285–298.

38. Mingozzi, F., and High, K.A. (2013). Immune responses to AAV vectors: overcoming barriers to successful gene therapy. Blood *122*, 23–36.

39. Lykken, E.A., Shyng, C., Edwards, R.J., Rozenberg, A., and Gray, S.J. (2018). Recent progress and considerations for AAV gene therapies targeting the central nervous system. J. Neurodev. Disord. *10*, 16.

40. Homs, J., Pagès, G., Ariza, L., Casas, C., Chillón, M., Navarro, X., and Bosch, A. (2014). Intrathecal administration of IGF-I by AAVrh10 improves sensory and motor deficits in a mouse model of diabetic neuropathy. Mol. Ther. Methods Clin. Dev. *1*, 7.

41. van de Beek, M.-C., Dijkstra, I.M.E., van Lenthe, H., Ofman, R., Goldhaber-Pasillas, D., Schauer, N., Schackmann, M., Engelen-Lee, J.Y., Vaz, F.M., Kulik, W., et al. (2016). C26:0-Carnitine Is a New Biomarker for X-Linked Adrenoleukodystrophy in Mice and Man. PLoS One *11*, e0154597.

42. Ranea-Robles, P., Galino, J., Espinosa, L., Schlüter, A., Ruiz, M., Calingasan, N.Y., Villarroya, F., Naudí, A., Pamplona, R., Ferrer, I., et al. (2022). Modulation of mitochondrial and inflammatory homeostasis through RIP140 is neuroprotective in an adrenoleukodystrophy mouse model. Neuropathol. Appl. Neurobiol. *48*, e12747.

43. Calcedo, R., Chichester, J.A., and Wilson, J.M. (2018). Assessment of Humoral, Innate, and T-Cell Immune Responses to Adeno-Associated Virus Vectors. Hum. Gene Ther. Methods *29*, 86–95.